Available online at www.sciencedirect.com

ScienceDirect

Mendeleev Commun., 2021, **31**, 465–468

Mendeleev Communications

Effect of heterovalent doping on photostimulated defect formation in $CsPbBr_3$

Ibrahim M. Sharaf,*[a,b] Anna V. Shurukhina,[a] Irina S. Komarova[a] and Alexei V. Emeline[a]

[a] *St. Petersburg State University, 198504 Peterhof, St. Petersburg, Russian Federation*
[b] *Department of Physics, Faculty of Science, Al-Azhar University, Assiut Branch 71542, Egypt. E-mail: isharaf90@yahoo.com*

DOI: 10.1016/j.mencom.2021.07.009

Two series of $CsPbBr_3$ perovskites doped with Bi or Ag were synthesized and investigated for photostimulated defect formation. It was demonstrated that the type and concentration of dopants strongly affect the absorption spectra and kinetics of photostimulated defect formation.

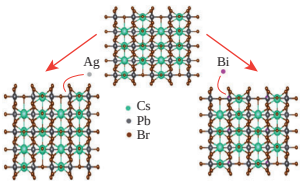

Keywords: halide perovskites, heterovalent doping, diffuse reflectance spectroscopy, photostimulated defect formation, photosensitive solids, photo-resistant solids.

Halide perovskites have suddenly received much attention since their first use as an absorber layer in solar cells in 2009.[1] In addition to record achievements in the efficiency of perovskite solar cells,[2] they have found wide application in various fields of optoelectronics.[3–6] Special attention in the research of halide perovskites is given to all-inorganic halide perovskite materials, such as $CsPbX_3$, because of their desirable optical properties and better environmental stability compared to hybrid organic–inorganic halide perovskites.[7–10] Due to outstanding electrical and optical properties such as tunable band gap across the entire visible region, high optical absorption coefficients, long carrier lifetime, high electron and hole mobility and defect tolerance, $CsPbX_3$ materials can be used in light-emitting diodes,[11] photodetectors,[12] memory devices,[13] radiation sensors[14] and others. Therefore, further improvement of functional properties is the primary goal of both fundamental and applied research of $CsPbX_3$ materials.

The classical method, which gives more freedom to modify the electronic and optical properties of semiconductor materials, is heterovalent doping, which is also readily applicable to $CsPbX_3$ perovskites.[15] A distinctive feature of heterovalent doping is that dopant ions introduce excess charge into the crystal lattice, which is compensated by forming intrinsic defects with a charge of the opposite sign to maintain crystal neutrality. Moreover, since the typical concentration of the dopant is close to or significantly exceeds the concentration of intrinsic defects in the pristine materials, newly formed intrinsic defects, which compensate for the excess charge of the dopant ions, play a significant role in establishing new electronic and optical characteristics of doped materials.

The basic building blocks of inorganic perovskite frameworks are $[PbX_{6/2}]$ octahedra connected by vertices along three orthogonal spatial dimensions. Moreover, it is the electronic states of the halide and lead that form the valence and conduction bands, respectively. Thus, controlled doping in the Pb position in octahedra can affect such fundamental properties as the position of the Fermi level, type of conductivity, lifetime and mobility of charge carriers, which provides an essential advantage for optoelectronic devices with electron transfer.[15–17] In particular, it was demonstrated that heterovalent doping with Bi^{3+} ions leads to a shift of the Fermi level to the conduction band, strong absorption at wavelengths exceeding the wavelength corresponding to the band gap energy and a change in conductivity to *n*-type.[18,19] In contrast, heterovalent doping with Ag^+ ions shifts the Fermi level towards the valence band and induces *p*-type conductivity.[20] These data mean that a significant redistribution of intrinsic defects is caused by heterovalent doping, as a result of which a particular type of defects becomes dominant in the perovskite structure, while other defects are negligible, depending on the type of dopant.

Under standard operating conditions, perovskite materials are in a highly non-equilibrium thermodynamic state due to electronic excitation induced by either absorbed light or applied voltage.[21,22] The interaction of free charge carriers or excitons caused by such excitation with lattice defects can significantly change both the type of defects and their energy distribution. In turn, these changes can affect both the electronic and optical behavior of the perovskite material.

In this work, we investigate the effect of photostimulated defect formation in $CsPbBr_3$ perovskite, depending on the nature of heterovalent dopant ions, Ag^+ or Bi^{3+}, as well as how the redistribution of intrinsic defect states caused by doping affects the mechanism of photostimulated defect formation. Another essential issue that we are trying to solve is to classify $CsPbBr_3$ perovskite as a photo-resistant or photosensitive material and elucidate the effect of heterovalent doping on its resistance (sensitivity) to light exposure[23–25] (for more details on photo-resistant and photosensitive materials, see Online Supplementary Materials). Likely, the presence of dopant ions can significantly alter the behavior of a material when exposed to light. Therefore, we also examine the effect of heterovalent doping with Ag^+ or Bi^{3+} on the photosensitivity of $CsPbBr_3$ perovskite.

Experimental details related to the synthesis procedure for both pristine and Ag- or Bi-doped $CsPbBr_3$ samples and data of X-ray diffraction analysis, scanning electron microscopy, X-ray photoelectron spectroscopy and diffuse reflectance spectroscopy are given in Online Supplementary Materials. The corresponding dopant contents are given in Table 1.

Table 1 Dopant content in $CsPbBr_3$ samples synthesized in this work.

Dopant	Content (at%)[a]			
Ag	0.038	0.088	0.29	0.44
Bi	0.088	0.18	0.26	0.43

[a] Average concentrations of dopants in $CsPbBr_3$ were determined on a Shimadzu ICPE-9000 ICP emission spectrometer.

Diffuse reflectance spectra $R(\lambda)$ were recorded in the spectral range of 436–800 nm at room temperature. Irradiation of samples in experiments on photostimulated defect formation was performed with an Hg lamp at a wavelength of 436 nm with an intensity of 11 ± 1 μW cm^{-2}. The diffuse reflectance spectra of doped and undoped $CsPbBr_3$ samples (Figure S5, see Online Supplementary Materials) exhibit the typical spectral response for pristine, Ag-doped and Bi-doped $CsPbBr_3$ perovskite. According to the measured spectra, Ag doping does not affect the fundamental light absorption of $CsPbBr_3$ and does not cause a change in the optical band gap (2.27–2.28 eV) [see Figure S5(*b*), inset], assuming a direct band-to-band transition. At the same time, Bi doping significantly extends the spectral range of absorption caused by the formation of defect states [see Figure S5(*a*), inset]. Accordingly, the absorption band with a maximum at 570 nm can be associated with intrinsic defects that compensate for the excess of the positive charge introduced by Bi^{3+} cations.

Irradiation of doped and undoped $CsPbBr_3$ leads to an increase in absorption in the spectral region corresponding to the extrinsic absorption of $CsPbBr_3$ associated with photoinduced defects. Figure 1 demonstrates the spectral changes *versus* irradiation time for the pristine $CsPbBr_3$. The spectral change is presented as the difference diffuse reflectance spectrum ΔR:

$$\Delta R = R_0 - R_t,$$

where R_0 is the diffuse reflectance spectrum of the initial state (before irradiation) of the sample, and R_t is the diffuse reflectance spectrum of the sample after irradiation for a given time t.

As shown in Figure 1, absorption by photoinduced defects manifests itself in the form of broad unresolved absorption spectra, indicating that these defects have a broad spectral and energy distribution of various defect states within the band gap of $CsPbBr_3$. The kinetics of the accumulation of photoinduced defects during irradiation [Figure 1(*b*)] demonstrates an exponential growth corresponding to equation S3 (see Online Supplementary Materials), which indicates that the mechanism of defect formation can be described by equations S1 and S2 and consists of trapping photogenerated charge carriers by pre-existing defects. In other words, pristine $CsPbBr_3$ perovskite exhibits irradiation behavior typical of photo-resistant solids.

Similar dependences obtained for $CsPbBr_3$ doped with Bi^{3+} are presented in Figures 2 and S6–S8. As seen from these experimental data, photoinduced defects in Bi-doped $CsPbBr_3$ exhibit a spectral response at longer wavelengths than pristine perovskite. The kinetics of photostimulated defect formation for all Bi-doped samples demonstrates a rather complex behavior and can be described as a rapid increase in the absorption of defects, followed by its rapid decline and reaching a plateau with a longer irradiation time.

Spectral variations and kinetic dependencies corresponding to the photostimulated defect formation in Ag^+ doped $CsPbBr_3$ are presented in Figures 3 and S9–S11. The results obtained indicate that doping with Ag causes a significant redistribution of defect states in $CsPbBr_3$ depending on the Ag content. Indeed, one can see that at the lowest Ag concentration, the absorption spectra and the kinetics of the accumulation of photoinduced defects are somewhat similar to those observed for the pristine perovskite sample. However, with increasing dopant concentration, a spectral redistribution is observed between the longer and shorter wavelength spectral regions (see Figures S9–S11). Finally, with the highest Ag content in perovskite, intense absorption at shorter wavelengths dominates, with a maximum at 575 nm (see Figure 3). Surprisingly, the spectral manifestation of the photoinduced absorption band in Ag-doped $CsPbBr_3$ is very similar to the absorption band of pre-existing defects in Bi-doped samples [see Figure S5(*a*), inset]. Moreover, an increase in the Ag content in $CsPbBr_3$ also leads to a change in the kinetic behavior in the spectral region at longer wavelengths from exponential growth, typical for photo-resistant solids (see equations S1–S3), to a linear dependence, which may indicate the formation of new defects in the crystal structure, which is typical for photosensitive solids (see equations S5 and S6).

Remarkably, the values of light absorption by photoinduced defects (recorded at $\lambda = 650$ nm), achieved during photoirradiation and corresponding to the plateau limits, decrease with an increase in the Bi content in the perovskite and become practically negligible at the highest dopant concentration [Figure 4(*a*)]. All these experimental results infer that pre-existing defects induced by Bi doping [Figure S5(*a*), inset] are very stable concerning the photostimulated defect formation. As a result, photoinduced defect formation has practically no effect on the absorption by intrinsic defects at shorter wavelengths and weakly changes the absorption at longer wavelengths. Moreover, the higher the Bi content, the lower the efficiency of the photostimulated defect formation. In other words, the photostimulated defect formation described by equations S1 and S2 is ineffective in Bi-doped $CsPbBr_3$ perovskites, which indicates their high photostability.

Figure 4(*b*) demonstrates the change in the efficiency of photostimulated defect formation, expressed as the initial rate of the absorption growth (dR/dt), with increasing Ag content. These

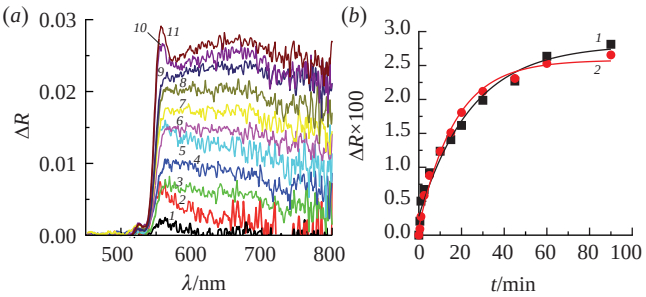

Figure 1 Time evolution of absorption by defects caused by irradiation at λ = 436 nm in pristine $CsPbBr_3$: (*a*) difference diffuse reflectance spectra after irradiation for (*1*) 0.5, (*2*) 1, (*3*) 2.5, (*4*) 5, (*5*) 10, (*6*) 15, (*7*) 20, (*8*) 30, (*9*) 45, (*10*) 60 and (*11*) 90 min and (*b*) kinetics of changes in diffuse reflectance recorded at wavelengths of (*1*) 560 and (*2*) 650 nm.

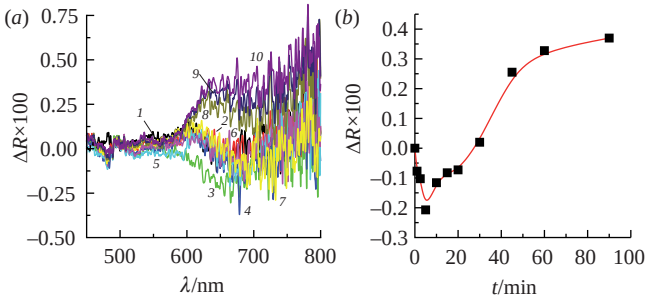

Figure 2 Time evolution of absorption by defects caused by irradiation at λ = 436 nm in $CsPbBr_3$ doped with Bi (0.43 at%): (*a*) difference diffuse reflectance spectra after irradiation for (*1*) 1, (*2*) 2.5, (*3*) 5, (*4*) 10, (*5*) 15, (*6*) 20, (*7*) 30, (*8*) 45, (*9*) 60 and (*10*) 90 min and (*b*) kinetics of changes in diffuse reflectance recorded at a wavelength of 650 nm.

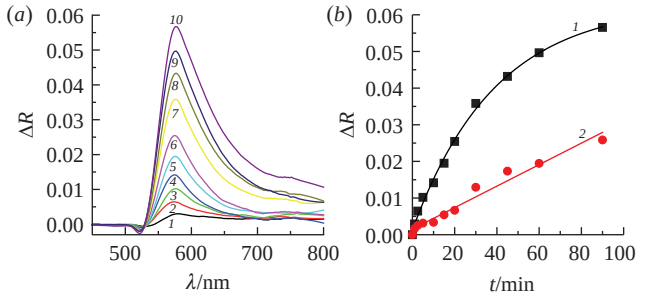

Figure 3 Time evolution of absorption by defects caused by irradiation at λ = 436 nm in $CsPbBr_3$ doped with Ag (0.44 at%): (*a*) difference diffuse reflectance spectra after irradiation for (*1*) 1, (*2*) 2.5, (*3*) 5, (*4*) 10, (*5*) 15, (*6*) 20, (*7*) 30, (*8*) 45, (*9*) 60 and (*10*) 90 min and (*b*) kinetics of changes in diffuse reflectance recorded at wavelengths of (*1*) 580 and (*2*) 650 nm.

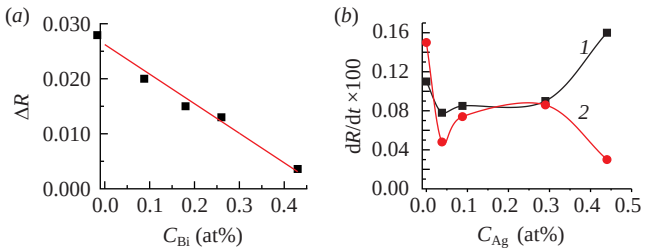

Figure 4 (*a*) The dependence of the limits of absorption by photoinduced defects on the Bi content in $CsPbBr_3$ and (*b*) the dependencies of the initial rate of photostimulated defect formation recorded at wavelengths of (*1*) 580 and (*2*) 650 nm on the Ag concentration in $CsPbBr_3$.

data also confirm that doping with Ag leads to a significant redistribution of pre-existing and, therefore, photoinduced defects in perovskite (otherwise, the dependence should be linear, since the higher the dopant content, the higher the defect formation efficiency should be).

In general, as mentioned at the beginning, heterovalent doping leads to an excess charge of the crystal lattice. In particular, the doping with Bi^{3+} ions in the Pb^{2+} positions results in excess of positive charge, and insertion of Ag^+ in octahedra instead of Pb^{2+} cations leads to an excess of negative charge. This excess charge causes a stronger interaction of the Br^- anions in octahedra with Bi^{3+} and a weaker interaction with Ag^+ cations. At the same time, heterovalent doping results in the formation of intrinsic defects with opposite charges to compensate for the charge of the dopant ions. Therefore, it can be expected that the compensation of the positive charge of Bi^{3+} should form intrinsic defects with a negative charge, such as cation vacancies (Cs^+ or Pb^{2+} vacancies) or interstitial Br^- anions. In turn, compensation for the negative charge introduced by cations of the Ag dopant into the lattice can be achieved by forming such defects as anion vacancies or interstitial cations. Accordingly, all these defects can participate in the photostimulated defect formation by trapping charge carriers or through the decay of excitons on defects, as described by equations S1 and S2. It should be noted that the Ag^+ cation in regular octahedron can also behave like a hole or an exciton trap when the hole or the hole component of the exciton is localized at the nearest Br^- anions. However, the localization of the positive charge of Bi^{3+} in octahedra does not create conditions for the localization of electrons or the electron component of excitons since the nearest Br^- anions cannot localize electrons. Consequently, an increase in the dopant concentration can lead to an increase in the concentration of specific defects, which compensate for the excess charge of the dopants and become the dominant type of defect in the perovskite structure.

Experimental results show that pristine $CsPbBr_3$ exhibits a broad distribution of all types of defect states, which leads to a wide unresolved absorption band. Doping with Bi^{3+} gives rise to intense absorption with a maximum at 575 nm, corresponding to specific defects that compensate for the excess positive charge. As shown from the experimental results on photostimulated defect formation, the initial states of these compensating defects are strongly stabilized by Bi dopant cations. They cannot effectively serve as traps for charge carriers, which leads to low efficiency of photostimulated defect formation. In contrast, Ag doping results in a high efficiency of photostimulated defect formation, which means that the defect states formed due to doping effectively trap the corresponding charge carriers or exciton components. However, a change in the Ag content in the perovskite material leads to a redistribution of compensating defects; that is, at different dopant concentrations, different types of compensating defects become dominant.

Since at the highest concentration of Ag dopant, the absorption spectrum of photoinduced defects looks similar to the absorption spectrum of initial compensating defects in Bi-doped perovskite, we can assume that the nature of photoinduced defects in Ag-doped perovskite is similar to the nature of initial defects in Bi-doped samples. Taking into account all possible types of defects and the nature of the kinetics of photostimulated defect formation in Ag-doped perovskite, which exhibits a linear dependence typical for photosensitive solids [Figure S5(*b*) and equations S5 and S6], we can assume the following mechanism of exciton decay:

$$Br^-_{Ag^+} + e^0 \rightarrow V_a + Br^-_{interst.} + e \rightarrow Br^-_{interst.} + F.$$

Here, the exciton is localized at the Br^- anion due to trapping the hole component by negatively charged octahedra containing the Ag^+ cation. Therefore, the localization of the exciton satisfies conditions 1 and 2 to form new defects in photosensitive solids (see Online Supplementary Materials). At the same time, the energy required to displace the Br^- anion from its usual position to the interstitial position ($Br^-_{interst.}$) is much lower in the octahedra containing the Ag^+ cation compared to regular octahedra. Consequently, this makes it possible to satisfy condition 3 for defect formation, according to which the exciton energy must be higher than the energy required to displace Br^-. A possible consequence of the proposed mechanism is the formation of interstitial states $Br^-_{interst.}$ and anionic vacancies V_a, which can trap an electron to form an F-type center. Note that interstitial states $Br^-_{interst.}$ are also possible candidates for the role of stable compensating defects in Bi-doped perovskite. Therefore, we assume that the similarity of the absorption spectra of stable initial defect states in Bi-doped $CsPbBr_3$ and photoinduced defect states in Ag-doped perovskite can be explained by the presence of interstitial states of Br^- anions.

In conclusion, we investigated the photostimulated defect formation in both pristine and Ag or Bi doped $CsPbBr_3$ perovskite. It was shown that photoinduced defects in pristine perovskite exhibit a broad energy and spectral distribution corresponding to various types of intrinsic defects. However, the doping with Bi or Ag leads, depending on the type of dopant, to a redistribution of intrinsic defects and the formation of dominant types of defect states to compensate for the excess charge of the corresponding dopant cations. Experimental results have shown that doping with Bi creates stable compensating defects ineffective in trapping charge carriers. Therefore, the efficiency of photostimulated defect formation in Bi-doped $CsPbBr_3$ is low, making the material a highly photo-resistant solid. On the contrary, doping with Ag results in a significant increase in the efficiency of photostimulated defect formation, and the results obtained indicate the possibility of the formation of new defect states characteristic of photosensitive solids.

This study was supported by the Saint Petersburg State University (project no. 73032813). The authors are grateful to the specialists of the SPbU Research Park from Resource centers 'Nanophotonics', 'X-Ray Diffraction Studies', 'Physical Methods of Surface Investigation', 'Nanotechnology' and 'Chemical Analysis and Materials Research' for their time, experience and helpful collaboration.

Online Supplementary Materials

Supplementary data associated with this article can be found in the online version at doi: 10.1016/j.mencom.2021.07.009.

References

1 A. Kojima, K. Teshima, Y. Shirai and T. Miyasaka, *J. Am. Chem. Soc.*, 2009, **131**, 6050.
2 *Best Research-Cell Efficiency Chart, the National Renewable Energy Laboratory, Golden, CO*, December 12, 2020. https://www.nrel.gov/pv/cell-efficiency.html.
3 M. Ahmadi, T. Wu and B. Hu, *Adv. Mater.*, 2017, **29**, 1605242.
4 Q. V. Le, H. W. Jang and S. Y. Kim, *Small Methods*, 2018, **2**, 1700419.
5 H. Dong, C. Zhang, X. Liu, J. Yao and Y. S. Zhao, *Chem. Soc. Rev.*, 2020, **49**, 951.
6 H. Wei and J. Huang, *Nat. Commun.*, 2019, **10**, 1066.
7 G. E. Eperon, G. M. Paternò, R. J. Sutton, A. Zampetti, A. A. Haghighirad, F. Cacialli and H. J. Snaith, *J. Mater. Chem. A*, 2015, **3**, 19688.
8 D. Zhang, S. W. Eaton, Y. Yu, L. Dou and P. Yang, *J. Am. Chem. Soc.*, 2015, **137**, 9230.
9 E. I. Marchenko, S. A. Fateev, A. A. Petrov, E. A. Goodilin and A. B. Tarasov, *Mendeleev Commun.*, 2020, **30**, 279.
10 Z.-J. Li, E. Hofman, A. H. Davis, A. Khammang, J. T. Wright, B. Dzikovski, R. W. Meulenberg and W. Zheng, *Chem. Mater.*, 2018, **30**, 6400.
11 S. A. Veldhuis, P. P. Boix, N. Yantara, M. Li, T. C. Sum, N. Mathews and S. G. Mhaisalkar, *Adv. Mater.*, 2016, **28**, 6804.
12 Y. Li, Z.-F. Shi, S. Li, L.-Z. Lei, H.-F. Ji, D. Wu, T.-T. Xu, Y.-T. Tian and X.-J. Li, *J. Mater. Chem. C*, 2017, **5**, 8355.
13 A. Kostopoulou, E. Kymakis and E. Stratakis, *J. Mater. Chem. A*, 2018, **6**, 9765.
14 V. B. Mykhaylyk, H. Kraus, V. Kapustianyk, H. J. Kim, P. Mercere, M. Rudko, P. Da Silva, O. Antonyak and M. Dendebera, *Sci. Rep.*, 2020, **10**, 8601.
15 B. Luo, F. Li, K. Xu, Y. Guo, Y. Liu, Z. Xia and J. Z. Zhang, *J. Mater. Chem. C*, 2019, **7**, 2781.
16 L. Xu, S. Yuan, H. Zeng and J. Song, *Materials Today Nano*, 2019, **6**, 100036.
17 R. Begum, M. R. Parida, A. L. Abdelhady, B. Murali, N. M. Alyami, G. H. Ahmed, M. N. Hedhili, O. M. Bakr and O. F. Mohammed, *J. Am. Chem. Soc.*, 2017, **139**, 731.
18 O. A. Lozhkina, A. A. Murashkina, V. V. Shilovskikh, Y. V. Kapitonov, V. K. Ryabchuk, A. V. Emeline and T. Miyasaka, *J. Phys. Chem. Lett.*, 2018, **9**, 5408.
19 A. L. Abdelhady, M. I. Saidaminov, B. Murali, V. Adinolfi, O. Voznyy, K. Katsiev, E. Alarousu, R. Comin, I. Dursun, L. Sinatra, E. H. Sargent, O. F. Mohammed and O. M. Bakr, *J. Phys. Chem. Lett.*, 2016, **7**, 295.
20 M. Abdi-Jalebi, M. Pazoki, B. Philippe, M. I. Dar, M. Alsari, A. Sadhanala, G. Divitini, R. Imani, S. Lilliu, J. Kullgren, H. Rensmo, M. Grätzel and R. H. Friend, *ACS Nano*, 2018, **12**, 7301.
21 Ch. Lushchik and A. Lushchik, *Raspad elektronnykh vozbuzhdenii s obrazovaniem defektov v tverdykh telakh* (*Decay of Electronic Excitations with Defect Formation in Solids*), Nauka, Moscow, 1989 (in Russian).
22 A. R. Silin' and A. N. Trukhin, *Tochechnye defekty i elementarnye vozbuzhdeniya v kristallicheskom i stekloobraznom SiO_2* (*Point Defects and Elementary Excitations in Crystalline and Vitreous SiO_2*), Zinatne, Riga, 1985 (in Russian).
23 A. Emeline, G. V. Kataeva, A. S. Litke, A. V. Rudakova, V. K. Ryabchuk and N. Serpone, *Langmuir*, 1998, **14**, 5011.
24 Ch. Lushchik and A. Lushchik, *Phys. Solid State*, 2018, **60**, 1487 (*Fiz. Tverd. Tela*, 2018, **60**, 1478).
25 A. Lushchik, Ch. Lushchik, E. Vasil'chenko and A. I. Popov, *Low Temp. Phys.*, 2018, **44**, 269 (*Fiz. Nizk. Temp.*, 2018, **44**, 357).

Received: 18th March 2021; Com. 21/6495